Article

Methyl Proton Contacts Obtained Using Heteronuclear Through-Bond Transfers in Solid-State NMR Spectroscopy

Antoine Loquet, Se#gole#ne Laage, Carole Gardiennet, Be#ne#dicte Elena, Lyndon Emsley, Anja Bo#ckmann, and Anne Lesage

J. Am. Chem. Soc., **2008**, 130 (32), 10625-10632 • DOI: 10.1021/ja801464g • Publication Date (Web): 16 July 2008

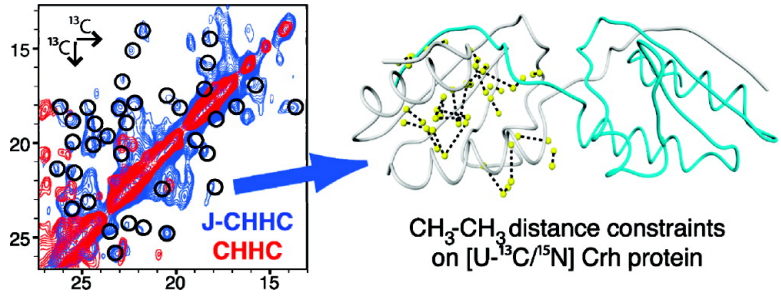

More About This Article

Additional resources and features associated with this article are available within the HTML version:

- Supporting Information
- Links to the 1 articles that cite this article, as of the time of this article download
- Access to high resolution figures
- Links to articles and content related to this article
- Copyright permission to reproduce figures and/or text from this article

View the Full Text HTML

J|A|C|S
ARTICLES

Published on Web 07/16/2008

Methyl Proton Contacts Obtained Using Heteronuclear Through-Bond Transfers in Solid-State NMR Spectroscopy

Antoine Loquet,[†] Ségolène Laage,[‡] Carole Gardiennet,[†] Bénédicte Elena,[‡] Lyndon Emsley,[‡] Anja Böckmann,*[,†] and Anne Lesage*[,‡]

Institut de Biologie et Chimie des Protéines, UMR 5086 CNRS/Université de Lyon 1, 7 passage du Vercors, 69367 Lyon, France, and Centre RMN à Très Hauts Champs, Université de Lyon, CNRS/ENS Lyon/UCB-Lyon 1, 5 rue de la Doua, 69100 Villeurbanne, France

Received February 27, 2008; E-mail: a.bockmann@ibcp.fr; Anne.Lesage@ens-lyon.fr

Abstract: A two-dimensional proton-mediated carbon−carbon correlation experiment that relies on through-bond heteronuclear magnetization transfers is demonstrated in the context of solid-state NMR of proteins. This new experiment, dubbed J-CHHC by analogy to the previously developed dipolar CHHC techniques, is shown to provide selective and sensitive correlations in the methyl region of 2D spectra of crystalline organic compounds. The method is then demonstrated on a microcrystalline sample of the dimeric protein Crh (2 × 10.4 kDa). A total of 34 new proton−proton contacts involving side-chain methyl groups were observed in the J-CHHC spectrum, which had not been observed with the conventional experiment. The contacts were then used as additional distance restraints for the 3D structure determination of this microcrystalline protein. Upon addition of these new distance restraints, which are in large part located in the hydrophobic core of the protein, the root-mean-square deviation with respect to the X-ray structure of the backbone atom coordinates of the 10 best conformers of the new ensemble of structures is reduced from 1.8 to 1.1 Å.

1. Introduction

Over the past few years, high-resolution solid-state NMR spectroscopy has emerged as an alternative technique to X-ray crystallography and solution-state NMR to obtain structural, dynamic, and biophysical insights at atomic resolution on noncrystalline or nonsoluble biological macromolecules.[1–5] Recent combined advances in instrumentation, NMR methodology, and notably sample preparation[6–11] have enabled high-resolution spectra of nonaligned biological samples to be obtained under conditions of magic angle spinning (MAS). Carbon-13 and nitrogen-15 spectral assignment strategies have emerged and have been successfully applied on a series of microcrystalline globular systems,[6,7,9–14] as well as on fibrils,[15–18] membrane proteins,[19–21] or the coat protein of intact viruses,[22] with secondary structure elements being simultaneously derived from the chemical shifts.

A major step in this field has been achieved with the demonstration, on the microcrystalline SH3 domain, that the three-dimensional (3D) global fold of a solid protein can be derived from MAS solid-state NMR spectroscopy.[23,24] The structure was calculated from a set of inter-residue $^{13}C-^{13}C$

[†] Institut de Biologie et Chimie des Protéines.
[‡] Centre RMN à Très Hauts Champs.

(1) McDermott, A. E. *Curr. Opin. Struct. Biol.* **2004**, *14*, 1–8.
(2) Opella, S. J.; Marassi, F. M. *Chem. Rev.* **2004**, *104*, 3587–3606.
(3) Tycko, R. *Curr. Opin. Struct. Biol.* **2004**, *14*, 96–103.
(4) Baldus, M. *Curr. Opin. Struct. Biol.* **2006**, *16*, 618–623.
(5) Böckmann, A. *Magn. Reson. Chem.* **2007**, *45*, S24–S31.
(6) Pauli, J.; Baldus, M.; van Rossum, B.; de Groot, H.; Oschkinat, H. *ChemBioChem* **2001**, *2*, 272–281.
(7) Böckmann, A.; Lange, A.; Galinier, A.; Luca, S.; Giraud, N.; Juy, M.; Heise, H.; Montserret, R.; Penin, F.; Baldus, M. *J. Biomol. NMR* **2003**, *27*, 323–339.
(8) Martin, R. W.; Zilm, K. W. *J. Magn. Reson.* **2003**, *165*, 162–174.
(9) Igumenova, T. I.; McDermott, A. E.; Zilm, K. W.; Martin, R. W.; Paulson, E. K.; Wand, A. J. *J. Am. Chem. Soc.* **2004**, *126*, 6720–6727.
(10) Igumenova, T. I.; Wand, A. J.; McDermott, A. E. *J. Am. Chem. Soc.* **2004**, *126*, 5323–5331.
(11) Franks, W. T.; Zhou, D. H.; Wylie, B. J.; Money, B. G.; Graesser, D. T.; Frericks, H. L.; Sahota, G.; Rienstra, C. M. *J. Am. Chem. Soc.* **2005**, *127*, 12291–12305.
(12) McDermott, A.; Polenova, T.; Bockmann, A.; Zilm, K. W.; Paulsen, E. K.; Martin, R. W.; Montelione, G. T. *J. Biomol. NMR* **2000**, *16*, 209–219.
(13) Marulanda, D.; Tasayco, M. L.; McDermott, A.; Cataldi, M.; Arriaran, V.; Polenova, T. *J. Am. Chem. Soc.* **2004**, *126*, 16608–16620.
(14) Pintacuda, G.; Giraud, N.; Pierattelli, R.; Böckmann, A.; Bertini, I.; Emsley, L. *Angew. Chem., Int. Ed.* **2006**, *46*, 1079–1082.
(15) Heise, H.; Hoyer, W.; Becker, S.; Andronesi, O. C.; Riedel, D.; Baldus, M. *Proc. Natl. Acad. Sci. U.S.A.* **2005**, *102*, 15871–15876.
(16) Ritter, C.; Maddelein, M. L.; Siemer, A. B.; Luhrs, T.; Ernst, M.; Meier, B. H.; Saupe, S. J.; Riek, R. *Nature* **2005**, *435*, 844–848.
(17) Siemer, A. B.; Ritter, C.; Ernst, M.; Riek, R.; Meier, B. H. *Angew. Chem., Int. Ed.* **2005**, *44*, 2441–2444.
(18) Siemer, A. B.; Ritter, C.; Steinmetz, M. O.; Ernst, M.; Riek, R.; Meier, B. H. *J. Biomol. NMR* **2006**, *34*, 75–87.
(19) Andronesi, O. C.; Becker, S.; Seidel, K.; Heise, H.; Young, H. S.; Baldus, M. *J. Am. Chem. Soc.* **2005**, *127*, 12965–12974.
(20) Kobayashi, M.; Matsuki, Y.; Yumen, I.; Fujiwara, T.; Akutsu, H. *J. Biomol. NMR* **2006**, *36*, 279–293.
(21) Etzkorn, M.; Martell, S.; Andronesi, O. C.; Seidel, K.; Engelhard, M.; Baldus, M. *Angew. Chem., Int. Ed.* **2007**, *46*, 459–462.
(22) Goldbourt, A.; Gross, B. J.; Day, L. A.; McDermott, A. E. *J. Am. Chem. Soc.* **2007**, *129*, 2338–2344.
(23) Castellani, F.; van Rossum, B.; Diehl, A.; Schubert, M.; Rehbein, K.; Oschkinat, H. *Nature* **2002**, *420*, 98–102.
(24) Castellani, F.; van Rossum, B.; Diehl, A.; Rehbein, K.; Oschkinat, H. *Biochemistry* **2003**, *42*, 11476–11483.

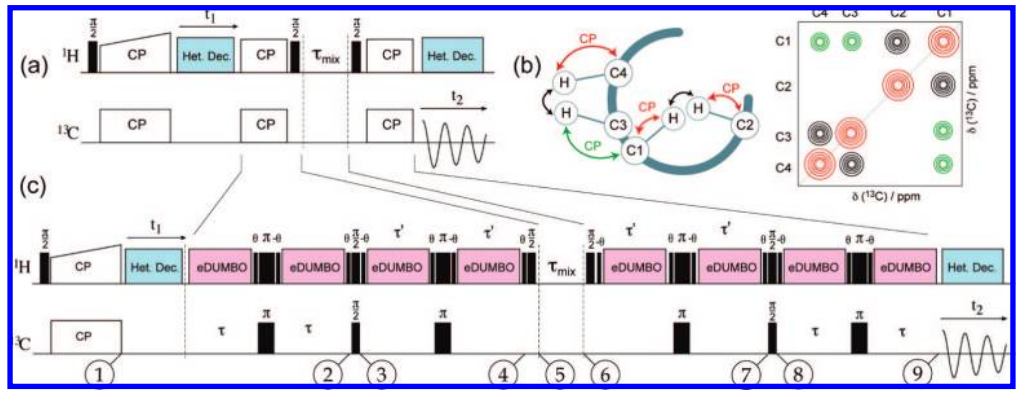

Figure 1. (a) Pulse sequence for the two-dimensional CHHC experiment allowing the observation of (^{1}H,^{1}H) contacts via carbon-13 correlations.[36,37] (b) Schematic representation of a 2D CHHC spectrum. The expected (^{13}C,^{13}C) cross-peaks are shown in black, while potential correlations due to nonselective cross-polarization transfers between C1 and H3 are indicated in green. (c) Pulse sequence for the two-dimensional J-CHHC experiment. The refocused INEPT blocks[28] replace the two short CP segments.

restraints obtained from proton-driven spin diffusion (PDSD) spectra of extensively labeled samples. A similar approach has led to the 3D structure determination of microcrystalline ubiquitin[25] and, more recently, of amyloid fibrils.[26] Restraints in solid proteins can be alternatively probed between proton spins. In small molecules, the direct observation of interproton correlations provides extended structural data.[27–29] With some notable exceptions,[30–32] in proteins, indirect detection schemes that encode proton−proton contacts in the normally better resolved ^{13}C or ^{15}N dimensions are used.[33–38] These are the so-called two-dimensional (2D) CHHC and NHHC experiments, which display ^{13}C−^{13}C or ^{15}N−^{13}C correlations that reflect internuclear contacts between protons in proximity to the heteronuclei and hence contain information about the 3D structure of the polypeptide chain. This methodology has been successfully applied to determine the 3D molecular structure of kaliotoxin,[39] a 38-residue peptide, and to probe structural features of a helical transmembrane protein complex.[40] We have also demonstrated that this type of experiment provides a sufficient number of ^{1}H−^{1}H distance restraints to refine at high-resolution the structure of the microcrystalline dimeric (2 × 10.4 kDa) Crh protein.[41,42] ^{1}H−^{1}H contacts clearly thus appear promising for structural data in solids.

The pulse sequence for the 2D CHHC experiment is shown in Figure 1a. The heteronuclear transfers between carbon and proton spins rely on cross-polarization (CP) steps of short duration,[36,37] typically of the order of 100 μs. A longitudinal mixing period enables polarization transfer between neighboring protons through spin diffusion. The resulting 2D map yields ^{13}C−^{13}C cross-peaks, whose buildup rates as a function of the longitudinal mixing time can be related to proton−proton internuclear distances. Although this experiment has been demonstrated to be useful, it does suffer from two limitations. The first one is related to the selectivity of the CP transfers. As they rely on through-space dipolar interactions, these transfers do not always provide magnetization transfer only between attached carbon and proton nuclei; consequently, despite the use of short contact times, this may lead to misleading cross-peaks in the 2D spectrum. This is schematically illustrated in Figure 1b, where we show that four extra correlations (in green) will be observed in the 2D CHHC spectrum (in addition to the expected ones, in black) when the magnetization is transferred between the non-chemically bonded C1 and H3 nuclei. While correlation peaks between nonattached pairs can provide valuable information on the conformation of the molecule, they may also greatly complicate the analysis of the 2D spectrum.

The second limitation of the 2D CHHC experiment concerns the sensitivity of the signals involving the methyl groups. As the proton−carbon dipolar couplings are reduced by the three-fold rotation of the CH_3 groups, the short contact times used for the CP steps prevent efficient polarization of these groups; as a consequence, the resulting spectrum displays weak or absent carbon−carbon correlations in the methyl region of the 2D spectrum (see below). Probing inter-residue methyl−methyl contacts is, however, of great interest for 3D structure determination, since they often represent highly useful long-range restraints in the hydrophobic core of the protein.

(25) Zech, S. G.; Wand, A. J.; McDermott, A. E. *J. Am. Chem. Soc.* **2005**, *127*, 8618–8626.
(26) Iwata, K.; Fujiwara, T.; Matsuki, Y.; Akutsu, H.; Takahashi, S.; Naiki, H.; Goto, Y. *Proc. Natl. Acad. Sci. U.S.A.* **2006**, *103*, 18119–18124.
(27) Brown, S. P.; Lesage, A.; Elena, B.; Emsley, L. *J. Am. Chem. Soc.* **2004**, *126*, 13230–13231.
(28) Elena, B.; Lesage, A.; Steuernagel, S.; Bockmann, A.; Emsley, L. *J. Am. Chem. Soc.* **2005**, *127*, 17296–17302.
(29) Elena, B.; Pintacuda, G.; Mifsud, N.; Emsley, L. *J. Am. Chem. Soc.* **2006**, *128*, 9555–9560.
(30) Agarwal, V.; Diehl, A.; Skrynnikov, N.; Reif, B. *J. Am. Chem. Soc.* **2006**, *128*, 12620–12621.
(31) Chevelkov, V.; Rehbein, K.; Diehl, A.; Reif, B. *Angew. Chem., Int. Ed.* **2006**, *45*, 3878–3881.
(32) Zhou, D. H.; Shea, J. J.; Nieuwkoop, A. J.; Franks, W. T.; Wylie, B. J.; Mullen, C.; Sandoz, D.; Rienstra, C. M. *Angew. Chem., Int. Ed.* **2007**, *46*, 1–5.
(33) Mulder, F. M.; Heinen, W.; van Duin, M.; Lugtenburg, J.; de Groot, H. J. M. *J. Am. Chem. Soc.* **1998**, *120*, 12891–12894.
(34) Wilhelm, M.; Feng, H.; Tracht, U.; Spiess, H. W. *J. Magn. Reson.* **1998**, *134*, 255–260.
(35) de Boer, I.; Bosman, L.; Raap, J.; Oschkinat, H.; de Groot, H. J. M. *J. Magn. Reson.* **2002**, *157*, 286–291.
(36) Lange, A.; Luca, S.; Baldus, M. *J. Am. Chem. Soc.* **2002**, *124*, 9704–9705.
(37) Lange, A.; Seidel, K.; Verdier, L.; Luca, S.; Baldus, M. *J. Am. Chem. Soc.* **2003**, *125*, 12640–12648.
(38) Reif, B.; van Rossum, B. J.; Castellani, F.; Rehbein, K.; Diehl, A.; Oschkinat, H. *J. Am. Chem. Soc.* **2003**, *125*, 1488–1489.
(39) Lange, A.; Becker, S.; Seidel, K.; Giller, K.; Pongs, O.; Baldus, M. *Angew. Chem., Int. Ed.* **2005**, *44*, 2089–2092.
(40) Ganapathy, S.; van Gammeren, A. J.; Hulsbergen, F. B.; de Groot, H. J. *J. Am. Chem. Soc.* **2007**, *129*, 1504–1505.
(41) Gardiennet, C.; Loquet, A.; Etzkorn, M.; Heise, H.; Baldus, M.; Böckmann, A. *J. Biomol. NMR* **2008**, *40*, 239–250.
(42) Loquet, A.; Bardiaux, B.; Gardiennet, C.; Malliavin, T. E.; Blanchet, C.; Nilges, M.; Baldus, M.; Bockmann, A. *J. Am. Chem. Soc.* **2008**, *130*, 3579.

Heteronuclear carbon−proton scalar couplings, although much smaller than the dipolar interactions, can be resolved in powder samples under MAS[43] and can be used to selectively transfer magnetization from carbon to proton spins.[44–46] We recently introduced a solid-state proton−carbon "insensitive nuclei enhanced by polarization transfer" (INEPT) correlation technique, where the magnetization is transferred from protons to bonded carbon nuclei under efficient homonuclear decoupling.[28] Here, we show that a 2D J-CHHC experiment, in which two refocused INEPT blocks replace the two short CP steps, provides selective and sensitive correlations in the methyl area of the resulting 2D spectrum, as demonstrated on the model sample L-isoleucine. We then show that this experiment can be successfully applied to a biological solid, namely the microcrystalline model protein Crh.[7] Analysis of the 2D J-CHHC spectrum reveals new proton-mediated correlations between methyl carbons not present in the conventional experiment, which we use as additional distance restraints in the 3D structure calculation of this solid protein. A significant improvement in the root-mean-square deviation (rmsd) of the backbone atom coordinates with respect the X-ray structure is obtained.

2. Pulse Scheme

The pulse sequence of the two-dimensional J-CHHC experiment, which is shown in Figure 1c, is built according to the same overall scheme as the 2D CHHC experiment[36,37] (Figure 1a): initial magnetization transfer from protons to carbons via a CP step (point ① in the figure); carbon-13 t_1 evolution under heteronuclear decoupling; back transfer of carbon magnetization to neighboring protons (until point ④); 90° ^{1}H flip-back pulse; longitudinal mixing time allowing for proton−proton magnetization exchange during τ_{mix}; 90° ^{1}H pulse and magnetization transfer to adjacent ^{13}C nuclei (from points ⑥ to ⑨); direct carbon detection. In the J-CHHC experiment, the magnetization transfer between proton and carbon pairs is, however, achieved by through-bond transfers using two refocused INEPT blocks,[28] which replace the two short CP steps of the CHHC experiment. These refocused INEPT blocks consist of two $\tau-\pi-\tau$ and $\tau'-\pi-\tau'$ periods under proton homonuclear decoupling. If the proton−proton decoupling sequence is efficient enough during these periods, fast magic-angle spinning then averages out chemical shift anisotropy and heteronuclear dipolar couplings. As the two simultaneous 180° pulses applied on the proton and carbon refocus the isotropic chemical shifts after 2τ and $2\tau'$, during these delays only J_{CH} couplings remain active and affect coherence transfer (the application of proton homonuclear decoupling leads to effective scaled J_{CH} couplings, the scaling factor being close to $1/\sqrt{3}$ and dependent on the employed decoupling scheme). For a pair of bonded (^{1}H,^{13}C) nuclei, after the first $\tau-\pi-\tau$ period, antiphase carbon coherence with respect to the attached proton is created (point ② in Figure 1). This antiphase coherence is converted by the two simultaneous 90° pulses into antiphase proton coherence (point ③), which is then refocused during the second $\tau'-\pi-\tau'$ period into in-phase proton magnetization (point ④). In the same way, the second refocused INEPT block will convert an in-phase proton magnetization (point ④) into the in-phase coherence of its attached carbon nucleus (point ⑨). The resulting 2D spectrum will display carbon−carbon correlations reflecting spatial proximities between their *bonded* protons.

3. Spin Dynamics Favors Methyl Groups

Figure 2 shows the theoretical evolution of carbon signal intensity in the J-CHHC experiment as a function of τ (transverse magnetization on the carbon spins) and τ' (transverse magnetization on the proton spins) evolution delays, during which the scalar couplings are active. In panels (a) and (b), the signal intensity is plotted for ^{13}C and ^{1}H transverse refocused linewidths Δ' and J_{CH} coupling values corresponding to the ideal liquid-state case, i.e., $\Delta'(^{13}C) = \Delta'(^1H) = 0$ Hz, and J_{CH}= 130 Hz. (The so-called refocused line width relevant for these experiments is defined as the broadening observed indirectly in the carbon or proton dimension of a spin−echo experiment under homonuclear decoupling and corresponds to a characteristic refocused transverse dephasing time T_2' according to $T_2 = 1/\pi\Delta'$.[47–49] In the liquid-state case, infinite transverse refocused coherence lifetimes are considered.) We note that, while the evolution of the carbon-13 signal intensity as a function of τ is dependent on carbon multiplicity, the evolution as a function of τ' is only modulated as $\sin(2\pi J_{CH}\tau')$.[2] In panels (c) and (d), the curves were calculated for the solid-state case, with a scaled J_{CH} coupling value of 75 Hz, and values for proton and carbon refocused linewidths were derived from T_2' measurements on the model compound L-isoleucine under high power (150 kHz radio frequency (RF) field) eDUMBO-1 homonuclear decoupling[49] (see Figure S1, Supporting Information). Figure 2c,d clearly shows that the evolution curves are strongly attenuated due to the transverse decay of carbon or proton magnetization during the successive echo periods in the solid-state case. As expected, the measured refocused linewidths $\Delta'(^{13}C)$ and $\Delta'(^1H)$ are significantly narrower (or the lifetimes of transverse coherences are longer) for rotating CH_3 groups than for more rigid (and therefore more strongly coupled) CH and CH_2 groups. (In other words, methyl groups are easier to decouple due to their intrisinc dynamics properties.) This leads to a stronger damping of the signal intensity for CH and CH_2 carbons as compared to methyl carbons. Note that, for these calculations, we considered only the attenuation due to the transverse decay of either the carbon or the proton magnetization in panels (c) and (d), respectively. However, both attenuations combine in the J-CHHC experiment, which further increases the expected discrepancy in sensitivity between CH and CH_2 groups on one hand and CH_3 groups in the other hand. It is therefore clear from this analysis that the J-CHHC experiment will work particularly well for methyl groups, exactly the groups for which the conventional experiment does not perform well. In contrast, CH and CH_2 groups are expected to yield poor sensitivity correlations under the current experimental conditions in the *J*-coupling-based CHHC experiment due to fast dephasing of transverse magnetization during the successive echo periods.

(43) Lesage, A.; Steuernagel, S.; Emsley, L. *J. Am. Chem. Soc.* **1998**, *120*, 7095–7100.
(44) Lesage, A.; Sakellariou, D.; Steuernagel, S.; Emsley, L. *J. Am. Chem. Soc.* **1998**, *120*, 13194–13201.
(45) Lesage, A.; Charmont, P.; Steuernagel, S.; Emsley, L. *J. Am. Chem. Soc.* **2000**, *122*, 9739–9744.
(46) Lesage, A.; Emsley, L. *J. Magn. Reson.* **2001**, *148*, 449–454.
(47) Lesage, A.; Bardet, M.; Emsley, L. *J. Am. Chem. Soc.* **1999**, *121*, 10987–10993.
(48) De Paepe, G.; Lesage, A.; Emsley, L. *J. Chem. Phys.* **2003**, *119*, 4833–4841.
(49) Elena, B.; de Paepe, G.; Emsley, L. *Chem. Phys. Lett.* **2004**, *398*, 532–538.

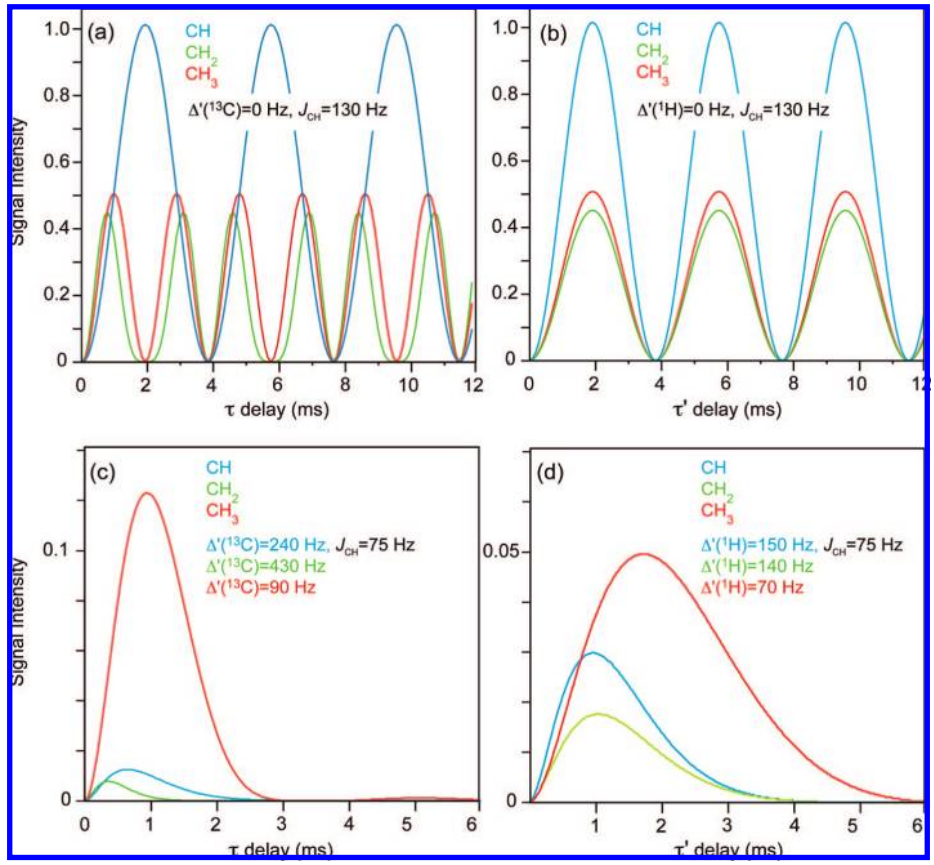

Figure 2. Theoretical curves for carbon signal intensity observed after the J-CHHC experiment. The curves were calculated as a function of both τ (in panels (a) and (c)) and τ' (in panels (b) and (d)). The simulations were performed using the SIMPSON software. In panels (a) and (b), signal intensity is plotted for ^{13}C and ^{1}H refocused linewidths Δ' and J_{CH} coupling values corresponding to the ideal liquid-state case, i.e., $\Delta'(^{13}C) = \Delta'(^{1}H) = 0$ Hz, and $J_{CH} = 130$ Hz. The curves follow theoretical behaviors given as follows: for a CH group, $\sin(2\pi J_{CH}\tau)^2 \sin(2\pi J_{CH}\tau')^2$; for a CH_2 group, $^1/_2 \sin(2\pi J_{CH}\tau')^2 \sin(4\pi J_{CH}\tau)^2$; for a CH_3 group, $^3/_{16} \sin(2\pi J_{CH}\tau')^2[\sin(2\pi J_{CH}\tau) + \sin(6\pi J_{CH}\tau)]^2$. In panels (c) and (d), the curves were calculated for the solid-state case, with a scaled J_{CH} coupling value of 75 Hz, and nonzero refocused linewidths. The Δ' values were obtained from measurements on L-isoleucine of proton and carbon transverse dephasing times T_2' under e-DUMBO homonuclear decoupling (see Supporting Information). The curves follow the theoretical behavior given above, but multiplied by an exponential decay according to $e^{-4\tau/T_2'^{C}}$ in (c) and $e^{-4\tau'/T_2'^{H}}$ in (d). In all cases, for each type of protonated group, the calculations as a function of τ were done using the τ' value that gives the best signal intensity and conversely.

4. Experimental Section

NMR Spectroscopy. The sample of fully ^{13}C-labeled L-isoleucine was purchased from Sigma and used without further recrystallization. The sample crystallizes with two molecules per unit cell. The assignment of the carbon-13 spectrum has been reported in a previous work.[47] All NMR experiments on this compound were performed at room temperature (293 K) on a Bruker Avance III 500 spectrometer (500 MHz proton resonance frequency), equipped with a standard 2.5 mm double-tuned MAS probe. Approximately 10 mg of sample was used. The MAS spinning frequency was set to 22 000 Hz. The 2D CHHC and J-CHHC spectra shown in Figure 3 were respectively acquired with a total of 64 and 256 scans and 96 t_1 increments, corresponding to a maximum t_1 evolution period of 4 ms and a recycle delay of 1.5 s. The difference in the number of scans between the two experiments has been taken into account in Figures 3 and 4 (i.e., the signal of the CHHC spectra has been multiplied by a factor of 2) as well as in all the discussion on signal-to-noise ratio. For both the CHHC and J-CHHC experiments, the contact time of the long CP step was 1 ms. For all CP steps, a ramped RF field centered at 80 kHz was applied on protons, while the carbon field strength was adjusted to obtain optimal signal. Two-pulse phase modulation (TPPM) heteronuclear decoupling[50] was applied during ^{13}C acquisition with a proton nutation frequency $\nu_1 = 100$ kHz. For 2D experiments, quadrature detection in ω_1 was achieved using the TPPI method on the carbon CP pulse.[51] For the J-CHHC experiments, continuous phase-modulated eDUMBO-1 proton homonuclear decoupling[49] was implemented during the heteronuclear transfer delays τ and τ', with a RF field strength of $\nu_1 = 150$ kHz. Each decoupling cycle ($\tau_C = 20$ μs) was divided into 200 phase steps of 100 ns each. The overall phase of eDUMBO-1 decoupling was adjusted to make the effective decoupling field lie in the (x,z) plane as described in ref 52. Short θ pulses (0.5 μs) rotate magnetization back into the (x,y) plane from the evolution plane perpendicular to the decoupling field (and toward for the "$-\theta$" pulses). The 180° pulse lengths on proton and carbon were set to 5 μs. A 256-step phase cycle was used in the J-CHHC experiment to select the proper coherence transfer pathway.

The [U-^{13}C,^{15}N]-labeled Crh protein sample was prepared as described previously.[7] The experiments on microcrystalline Crh were recorded on a Bruker Avance III 500 spectrometer (500 MHz frequency for protons). The one-dimensional spectrum in Figure 5 was obtained with a 4 mm MAS probe at a spinning frequency of 12.5 kHz. The RF field for eDUMBO-1 homonuclear decoupling was 100 kHz (the decoupling cycle of 30 μs was divided into 300

(50) Bennett, A. E.; Rienstra, C. M.; Auger, M.; Lakshmi, K. V.; Griffin, R. G. *J. Chem. Phys.* **1995**, *103*, 6951.

(51) Marion, D.; Wüthrich, K. *Biochem. Biophys. Res. Commun.* **1983**, *113*, 967–974.

(52) Lesage, A.; Sakellariou, D.; Hediger, S.; Eléna, B.; Charmont, P.; Steuernagel, S.; Emsley, L. *J. Magn. Reson.* **2003**, *63*, 105–113.

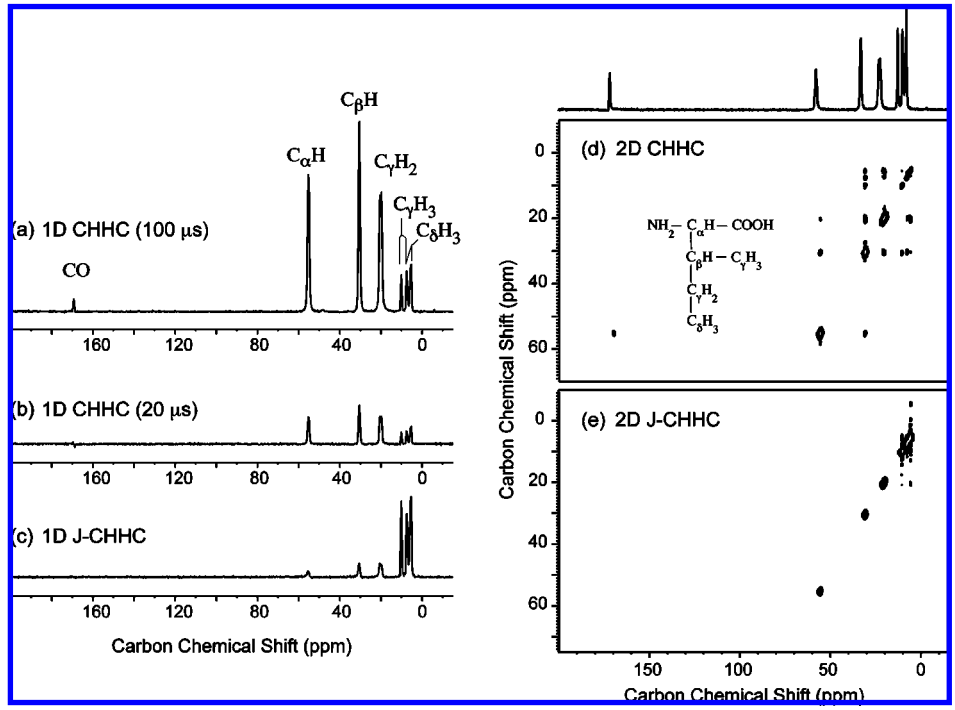

Figure 3. One-dimensional CHHC spectra of [U-^{13}C]-L-isoleucine acquired with short CP steps of 100 μs (a) and 20 μs (b), and comparison with a one-dimensional J-CHHC spectrum (c). In each case the mixing time was zero. Delays of 1.2 and 1.4 ms were respectively set for the τ and τ' periods for optimum efficiency on the CH_3 groups. Two-dimensional CHHC (d) and J-CHHC (e) spectra of [U-^{13}C]-L-isoleucine also with zero mixing times. For the CHHC spectrum, the contact times for the two short CP segments were set to 100 μs. All spectra were recorded with a proton longitudinal mixing time equal to zero.

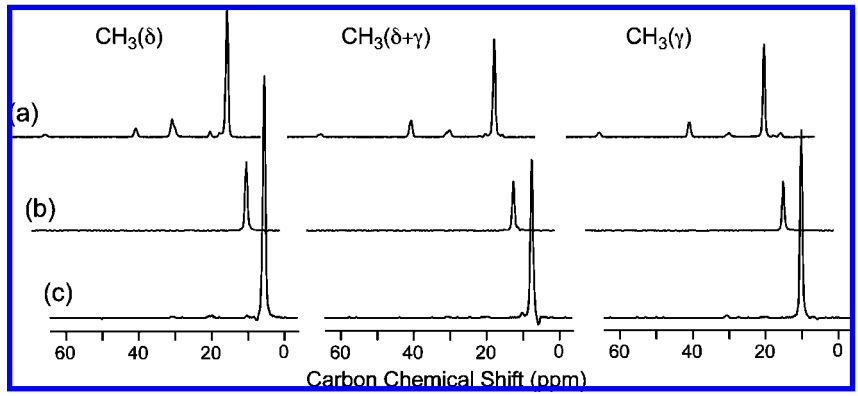

Figure 4. One-dimensional ω_2 rows extracted from 2D CHHC correlation spectra with short CP segments of 100 μs (a) and 20 μs (b), and from a J-CHHC (c) correlation spectrum on [U-^{13}C]-L-isoleucine. The experimental conditions were the same as in Figure 3 (proton longitudinal mixing time set to zero). The traces correspond to the three distinct methyl resonances. (Note that, although there are two molecules in the unit cell, only three distinct methyl resonances are observed in the 1D CPMAS carbon-13 spectrum of fully enriched L-isoleucine.) We note that very weak cross-peaks are visible in the traces extracted from the J-CHHC experiment (c), which may result from the imperfect suppression of the dipolar couplings or from multiple-bond through-bond transfers.

phase steps of 100 ns), while SPINAL-64 heteronuclear decoupling was applied at 80 kHz. A total of 96 t_1 increments with 512 scans each were acquired with a recycle delay of 3 s, giving a total acquisition time of 3 days. The 2D CHHC spectrum of Figure 5 was acquired with the same probe at a spinning frequency of 11 kHz. A total of 96 t_1 increments with 320 scans each were acquired with a recycle delay of 3 s. The Hartmann−Hahn matching for the short CP segments (contact time of 150 μs) were carefully adjusted to obtain maximum signal. The longitudinal mixing time for proton−proton magnetization exchange was set to 400 μs for both spectra, and the temperature of the sample was regulated at 273 K (actual sample temperature about 5 °C). To take into account the difference in the number of scans between the two 2D experiments, the signal of the CHHC spectrum was multiplied by 1.26 in Figure 5. All pulse programs and phase cycles are available from the authors.

Structure Calculations of the Dimer Crh Protein. Manual peak picking was realized using the Sparky program, version 3.100 (T. D. Goddard and D. G. Kneller, University of California). Torsion angles were predicted from N, Cα, Cβ, and C′ chemical shifts[7] using the TALOS[53] software. Dihedral angle predictions involving 56 out of 85 residues were considered as "good" by TALOS and used as dihedral constraints with error margins given by the program. The ^{1}H−^{1}H distance restraints extracted from the J-CHHC

(53) Cornilescu, G.; Delaglio, F.; Bax, A. *J. Biomol. NMR* **1999**, *13*, 289–302.

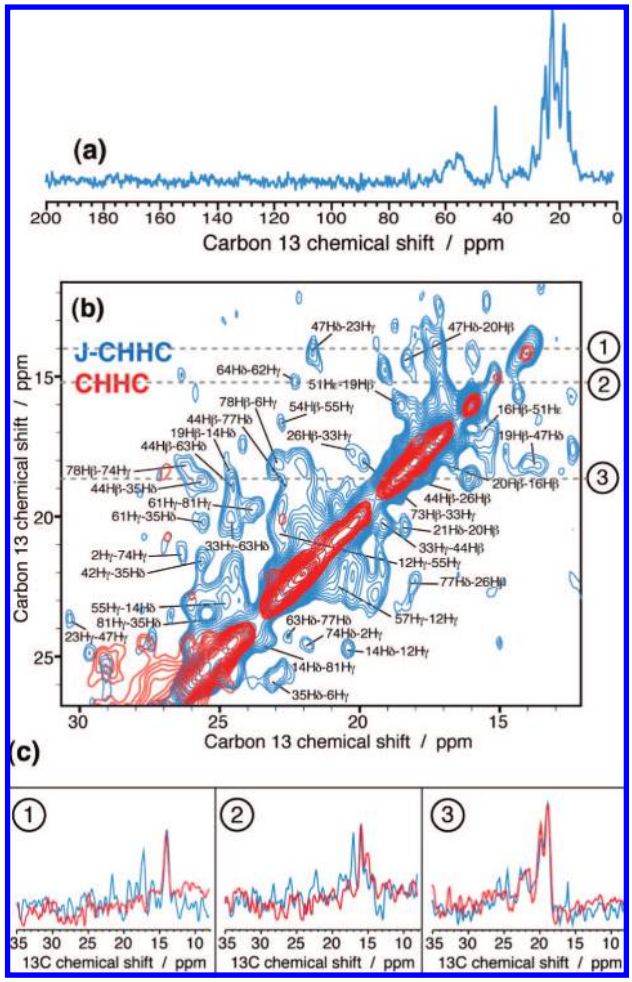

Figure 5. (a) One-dimensional J-CHHC carbon-13 spectra acquired on uniformly ^{13}C- and ^{15}N-labeled microcrystalline Crh protein. The experiment was recorded at $\omega_R = 12.5$ kHz using a 4 mm rotor. The mixing time was fixed to zero. (b) Extracts in the carbon-13 methyl region of two-dimensional CHHC (in red) and J-CHHC (in blue) spectra on uniformly ^{13}C- and ^{15}N-labeled microcrystalline Crh protein. The longitudinal proton mixing time was identical (400 μs) for the two experiments. The assignment of the additional cross-peaks observed in the J-CHHC spectrum was performed using the single-crystal structure of the dimeric Crh protein (PDB entry 1MU4[58]). The correlations in the other areas of the J-CHHC spectrum are too low to be exploitable. Note that unassigned cross-peaks correspond to either ambiguous correlations (containing two or more correlations) or ntra-residue methyl−methyl proximities. (c) One-dimensional traces extracted along ω_2 from the 2D CHHC (in red) and J-CHHC (in blue) spectra. Diagonal peaks were normalized to the same intensity.

spectrum were identified by using the X-ray crystallographic structure of Crh (PDB entry 1MU4) as described previously[42] and were defined by a unique distance target of 3.5 Å, an upper bound of 5 Å, and a lower bound of 1.8 Å. For the CHHC and NHHC spectra, we used the same input set of distance restraints as previously published.[42]

To calculate the structure of the dimeric Crh protein, we used the program XPLOR-NIH.[54] The calculations started with the generation of a random monomer structure with good local geometry, followed by duplication of the monomeric unit and rotation of 180° around one of the internal axes to obtain a symmetric dimer. For each of the 100 random dimer conformers generated, calculations proceeded through three stages: (i) a high-temperature searching phase at 2000 K (20 000 steps), (ii) an annealing stage from 2000 to 100 K in temperature steps of 50 K, and (iii) a final gradient minimization of 400 cycles of Powell minimization. During the calculations, a pseudoenergy term, the noncrystallographic symmetry (NCS) restraint,[55] was used to keep the two monomer units superimposable by minimizing the atomic rmsd between the two monomer units which form the dimer. The two-fold symmetry was enforced through distance symmetry restraints.[56] An ensemble of 10 conformers was selected according to the lowest energy. The 10 selected conformers were aligned on the backbone atoms using MOLMOL 2K.2.[57]

5. Experimental Results on L-Isoleucine

Figure 3 compares one- and two-dimensional CHHC and J-CHHC spectra of a crystalline powder of a fully ^{13}C-labeled sample of L-isoleucine. The 1D CHHC spectra were recorded with short CP contact times of 100 (a and d) and 20 (b) μs. We first observe that, as expected from the above simulations, the CH and CH_2 resonances are strongly attenuated in the 1D J-CHHC experiment (Figure 3c), while a significant gain in sensitivity is obtained for the methyl groups when compared with the 1D CHHC spectra (Figure 3a,b). We also observe in the spectrum of Figure 3a that the carbonyl peak at 170 ppm is clearly visible, reflecting the fact that magnetization transfers in this experiment are indeed not perfectly selective, as discussed above; i.e., they do not occur exclusively within bonded carbon and proton pairs but also involve nuclei that are farther away. In contrast, the carbonyl peak is not observed in the 1D J-CHHC experiment as expected for a nonprotonated carbon. To ensure the same selectivity with regard to the carbonyl peak, we found experimentally that contact times as short as 20 μs have to be employed in the CHHC experiment (b). *This gain in selectivity, however, compromises the overall spectral sensitivity of the CHHC spectrum* (although the CH and CH_2 resonances are still more intense than in the J-CHHC spectrum). The 2D map of Figure 3d illustrates more clearly the fact that the dipolar CHHC experiment offers only a partial selectivity. Despite the use of a zero longitudinal mixing period, several correlations are observed between the methyl carbons, for example, and the Cβ and Cδ carbons, albeit relatively weak compared to the main diagonal peak (see Figure 4).

The improvement in sensitivity in the methyl region of the spectra can be quantified more precisely from ω_2 traces extracted from the 2D J-CHHC and CHHC spectra (Figure 4). A gain of about a factor of 2 in sensitivity is observed for the J-CHHC experiment (c) by comparison with the CHHC experiment recorded with short CP steps of 100 μs (a). This gain reaches a factor of 4 when the comparison is made with the more selective CHHC experiment recorded with 20 μs CP contact times (b). This difference in sensitivity between the two methods is related both to the intrinsically good performance of the J-CHHC experiment with respect to methyl groups, as discussed in section 4, and to the fact that the short contact times used for the dipolar CHHC experiment compromise efficient through-space polarization transfer within the fast-rotating methyl groups, as discussed above.

(54) Schwieters, C. D.; Kuszewski, J. J.; Tjandra, N.; Clore, G. M. *J. Magn. Reson.* **2003**, *160*, 65–73.
(55) Brünger, A. T.; Adams, P. D.; Clore, G. M.; DeLano, W. L.; Gros, P.; Grosse-Kunstleve, R. W.; Jiang, J. S.; Kuszewski, J.; Nilges, M.; Pannu, N. S.; Read, R. J.; Rice, L. M.; Simonson, T.; Warren, G. L. *Acta Crystallogr. D: Biol. Crystallogr.* **1998**, *54*, 905–921.
(56) Nilges, M. *Proteins* **1993**, *17*, 297–309.
(57) Koradi, R.; Billeter, M.; Wüthrich, K. *J. Mol. Graphics* **1996**, *14*, 51–55.

6. Application to the Microcrystalline Crh Protein

The practicability of the J-CHHC experiment to improve the detection of proton−proton methyl contacts has been probed on a larger and more complex biological system. Figure 5 shows experimental data recorded for a microcrystalline sample of Crh,[7] an 85-residue dimeric protein involved in catabolite repression. We have recently demonstrated[42] the possibility to obtain high-resolution 3D structures of this protein in the solid state by using ^{1}H−^{1}H distance restraints derived from both CHHC and NHHC experiments. As discussed above for L-isoleucine, we have found experimentally in these studies that ^{1}H−^{1}H contacts involving methyl protons are under-represented in the 2D spectra of CHHC experiments.[41] Thus, among the restraints identified from CHHC spectra, only 15 out of 643 were methyl−methyl contacts.[42] Methyl-containing amino acid residues (Ala, Ile, Leu, Met, Thr, and Val) are, however, ubiquitous in proteins (38 amino acids out of 85 in Crh) and therefore are expected to provide a large pool of possible structural information. Moreover, methyl−methyl contacts are particularly strong restraints for structure calculations since they often involve contacts between side chains that are buried in the hydrophobic core and that constitute key junctions between the structural elements of the protein.

Figure 5a shows the one-dimensional J-CHHC spectrum recorded on [U-^{13}C/^{15}N]-labeled Crh with a MAS spinning frequency of 12.5 kHz (no longitudinal proton mixing time). It shows that the signal intensity concentrates, as predicted above, in the methyl carbon resonances, between 12−30 ppm. An additional strong peak at 42 ppm is clearly observed, which can be assigned to the Cϵ resonances of the lysine residues (K37, K40, K50, and K76). The presence of this resonance is explained by the greater flexibility of the lysine side chains, which partially reduces the dipolar interactions and leads to longer transverse dephasing times of proton and carbon coherences (in a similar manner as for methyl groups). Figure 5b shows the methyl region of the corresponding 2D J-CHHC spectrum (in blue), superimposed with a dipolar CHHC spectrum recorded with the same spin diffusion mixing period ($\tau_{mix} = 400\ \mu$s; this value was chosen to favor methyl contacts for which dipolar interactions are weaker). Numerous additional cross-peaks are clearly observed in this part of the J-CHHC correlation map as compared to the dipolar version. Using an assignment strategy based on the use of the crystal structure of the Crh dimeric protein as a homology model (described in detail in ref 41), we assigned 34 ^{1}H−^{1}H contacts observed in the J-CHHC spectrum which all involve at least one methyl proton. These contacts divide themselves into two sequential contacts ($|i - j| = 1$), three medium-range contacts ($1 < |i - j| < 5$), and 29 long-range contacts ($|i - j| \geq 5$). Among the long-range contacts, six involve ^{1}H−^{1}H proximities between the two monomers. A list of the proton−proton contacts observed in the methyl area of the 2D J-CHHC spectrum is given in the Supporting Information. Among the 34 contacts, 32 are methyl−methyl proximities, ranging from 2.06 to 4.96 Å according to the X-ray structure (the complete list of distance contacts observed in the J-CHHC spectrum is given in Figure S2, Supporting Information). Figure 5c shows a comparison of one-dimensional traces extracted from the 2D CHHC (in red) and J-CHHC (in blue) spectra. The J-CHHC spectrum shows methyl−methyl correlations with reasonable sensitivity in this protein sample, especially when compared to the sensitivity of these correlations in the dipolar CHHC spectrum.

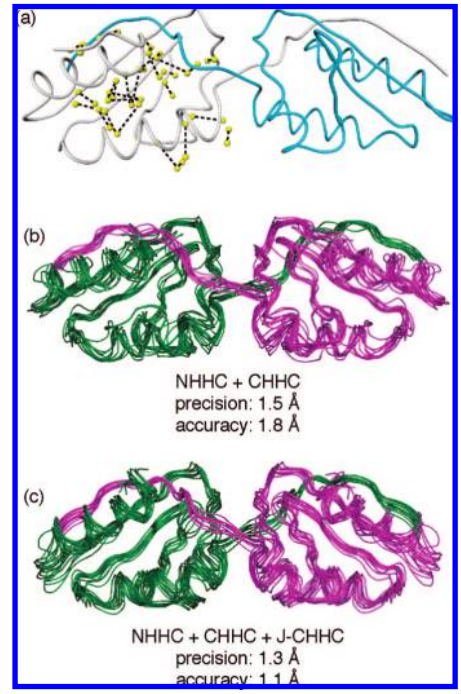

Figure 6. (a) Single-crystal structure of the dimeric Crh protein (PDB entry 1MU4) showing, for one monomer, the 34 ^{1}H−^{1}H distance contacts identified from the 2D J-CHHC spectrum of Figure 5. (b) Structure ensemble for the 10 best conformers of the dimeric Crh protein calculated using ^{1}H−^{1}H distance restraints obtained only from NHHC and CHHC experiments. (c) New structure ensemble for the 10 best conformers calculated using, in addition to the ^{1}H−^{1}H distance restraints employed in (b), the proton−methyl contacts derived form the J-CHHC spectrum of Figure 5. Precision and accuracy values are given for the backbone heavy atoms of residues [V2..Q82].

Figure 6a shows the distance contacts identified in the J-CHHC spectrum on the 3D crystal structure of Crh. As expected, the majority of these contacts are located in the hydrophobic core of the protein and therefore provide strong structural constraints for the 3D structure determination. In addition, six contacts are inter-monomeric proton proximities involving residues located in the β-strands involved in domain swapping and, as such, are expected to be useful structural constraints in the refinement of the dimeric structure.

To evaluate the benefit of the structural information encoded in these new ^{1}H−^{1}H contacts, we calculated the structure of dimeric Crh with two different input data sets: one with the ^{1}H−^{1}H distance restraints identified previously[42] from CHHC and NHHC spectra (192 distance restraints), and a second one adding the 34 new contacts involving methyl protons and observed in the J-CHHC spectrum. Only one distance class was used to encode the ^{1}H−^{1}H distance restraints. Figure 6b shows the 10 best conformers obtained from the first set of constraints (according to the protocol described in the Experimental Section). The 10 best conformers obtained with the second set of constraints, i.e., upon addition of the contacts derived from the J-CHHC experiment, are shown in Figure 6c. We clearly observe that the introduction of these new constraints in the calculations leads to a significant improvement of the convergence of the structures and therefore of the quality of the structure ensemble. Thus, the rmsd for the backbone heavy atoms of the 10 best conformers (precision) decreases from 1.5 to 1.3 Å when the constraints obtained from the J-CHHC experiment are added to the calculations. Similarly, the rmsd with respect to the single-crystal structure[58] (accuracy) notably

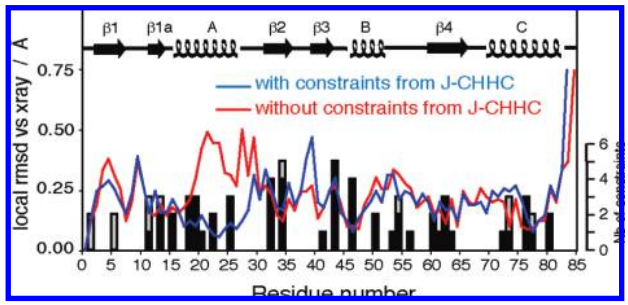

Figure 7. Variation of the local rmsd between the X-ray structure of the Crh protein and the 10 best solid-state NMR conformers calculated with (in blue) and without (in red) $^1H-^1H$ distance restraints derived from the 2D J-CHHC spectrum. The $^1H-^1H$ distance restraints identified in the J-CHHC spectrum are shown as bars, in black for intra-monomeric contacts and in gray for inter-monomeric contacts.

drops from 1.8 to 1.1 Å. This remarkable improvement is related to the fact that, as pointed out above, most of the constraints derived from the J-CHHC experiment are long-range constraints involving side-chain protons of the hydrophobic core. This effect is further reinforced by the presence of six inter-monomeric constraints, which constrain the dimeric topology of the protein.

As shown in Figure 7, the major improvement in the accuracy of the solid-state NMR structure calculated with the J-CHHC constraints is located in the protein segment 16−26, which corresponds to the α-helix A. Our previous analysis of CHHC and NHHC spectra[42] had revealed that this segment did suffer from a lack of $^1H-^1H$ distance restraints, and particularly long-range ones to connect α-helix A to the rest of the structured elements of the protein. This gain in accuracy here is understandable from the large number (10 with 8 long-range) of side-chain $^1H-^1H$ contacts involving the α-helix A added by the J-CHHC. This observation is consistent with a recent study of de Groot and co-workers,[40] who pointed out that the $^1H-^1H$ spin diffusion approach is more efficient to probe contacts between helical regions and other structured elements than 2D carbon-13 proton-driven spin diffusion data, with this effect being here further reinforced by the ability of the J-CHHC experiment to enhance the detection of side-chain methyl protons. Finally, we remark that the improvement in the backbone local rmsd is not only obtained for the residues for which new $^1H-^1H$ distance restraints have been found.

7. Conclusion

We introduced a new proton-mediated NMR carbon−carbon correlation technique, the J-CHHC experiment, based on selective heteronuclear through-bond transfers. We show that this experiment provides, with high sensitivity, methyl−methyl distance restraints for protein structure determination in the solid state. The experiment works well for groups with some degree of restricted mobility. Hence the good performance for methyl groups, but the experiment presented here should also prove highly useful in cases where the protons are isotopically diluted (as is the case, for example, in perdeuterated, methyl-protonated samples) and where longer transverse coherence lifetimes are expected, or when flexible protein segments are involved where local dynamics partly average out the dipolar couplings, and for which the detection of distance contacts via dipolar CHHC experiments is challenging. The J-CHHC experiment relies on the application of efficient, state-of-the-art, homonuclear decoupling techniques. This research area should experience major advances in the coming years, notably with the introduction of new hardware, such as very fast MAS and high-RF capability probes. These developments will lead to a consequent sensitivity improvement of the J-CHHC experiment, in particular with respect to the CH and CH_2 carbon resonances, which are only poorly correlated using current methodology. The sensitivity of the J-CHHC experiment could be alternatively improved by implementing proton-detected experiments, as was recently done for other types of correlation methods.[59]

The J-CHHC experiment has been demonstrated here to be a useful tool *complementary* to the conventional dipolar CHHC experiment. In the more general context of 3D structural investigations of biological solids, the methyl−methyl contacts extracted from the J-CHHC experiment will form apool of restraints complementary to restraints obtained from other techniques involving dipolar recoupling of many spins, like PDSD or TSAR[60] experiments, as has been demonstrated for nitrogen−methyl carbon restraints obtained using the SCT-TEDOR method[61] or for the carbonyl side-chain restraints extracted from the recently developed HBR2 technique.[62]

Acknowledgment. The authors thank Marc Baldus for stimulating them to do this work with interesting discussions in 2002. The authors also acknowledge useful discussions with G. Pintacuda. This work was funded in part by CNRS and the French research ministry (ANR JCJC JC05_44957, ACI Biologie cellulaire moléculaire et structurale), and by the Access to Research Infrastructures activity in the sixth Framework Programme of the EC (Contract No. RII3-026145, EU-NMR).

Supporting Information Available: Measurements of the proton (Figure S1a) and carbon (Figure S1b) transverse refocused lifetimes T_2' on L-isoleucine under homonuclear eDUMBO-1 decoupling; distance restraints identified in the 2D J-CHHC spectrum of the [U-$^{13}C/^{15}N$]-labeled Crh protein (Figure S2). This material is available free of charge via the Internet at http://pubs.acs.org.

JA801464G

(58) Juy, M.; Penin, F.; Favier, A.; Galinier, A.; Montserret, R.; Haser, R.; Deutscher, J.; Böckmann, A. *J. Mol. Biol.* **2003**, *332*, 767–776.
(59) Zhou, D. H.; Shah, G.; Cormos, M.; Mullen, C.; Sandoz, D.; Rienstra, C. M. *J. Am. Chem. Soc.* **2007**, *129*, 11791.
(60) Lewandowski, J. R.; De Paepe, G.; Griffin, R. G. *J. Am. Chem. Soc.* **2007**, *129*, 728–729.
(61) Helmus, J. J.; Nadaud, P. N.; Höfer, N.; Jaroniec, C. P. *J. Chem. Phys.* **2008**, *128*, 052314.
(62) Peng, X. H.; Libich, D.; Janik, R.; Harauz, G.; Ladizhansky, V. *J. Am. Chem. Soc.* **2008**, *130*, 359–369.